Solidification of Tilted-Lamellar Eutectic Grains with a Crystal Mosaicity: A Numerical Simulation Approach

S. Akamatsu, K. Saravanabavan, M. Medjkoune, S. Bottin-Rousseau

Solidification of tilted-lamellar eutectic grains with a crystal mosaicity: a numerical-simulation approach

S. Akamatsu,[1,*] K. Saravanabavan,[1] M. Medjkoune,[1,2] and S. Bottin-Rousseau[1]

[1] *Sorbonne Université, CNRS-UMR 7588, Institut des NanoSciences de Paris, case courrier 840, 4 place Jussieu, 75252 Paris Cedex 05, France*

[2] *Aix Marseille Univ., Université de Toulon, CNRS, IM2NP, Marseille, France*

In regular binary eutectic alloys, the shape of two-phase solidification microstructures varies between neighboring eutectic grains. This occurs in particular in alloys that present special orientation relationships (ORs) between the two kinds of crystals. In practice, eutectic grains most often present spatial variations of the crystal orientation of a few degrees. The consequences of this "mosaicity" on the growth dynamics are not clear. We present the first steps of a numerical investigation (boundary-integral method) of the dynamics of the so-called locked-lamellar patterns in the presence of a mosaicity. Realistic alloy parameters were used. We simulated a few pairs of lamellae (periodic boundary conditions) with a smoothly modulated anisotropy of the interphase boundaries in the solid. The pattern evolves then toward a steady-state regime with a uniform lamellar tilt angle, but a spatial modulation of the lamella width.

I. INTRODUCTION

The formation of coupled-growth patterns during the directional solidification of nonfaceted eutectic alloys (regular eutectics) is primarily governed by solute diffusion in the liquid and local-equilibrium capillary effects at the solid-liquid interface [1, 2]. This dynamics gives rise to the freezing of various composite microstructures with more or less complex spatial arrangements in the bulk material, depending on alloy characteristics, control parameters and the experimental path [3]. The shape of eutectic solidification microstructures can also depend on the orientation of the crystals of the different eutectic solid phases. This has been evidenced experimentally for a long time in lamellar eutectics that present special orientation relationships (ORs) between the two eutectic solids [4, 5]. In a given eutectic grain, the lamellae often grow tilted, with a fixed inclination with respect to the main solidification axis (lamellar locking). This particular inclination is very close to that of dense coincidence planes that characterize an OR. Importantly, an interphase boundary that aligns, in the solid, with a dense coincidence plane realizes a minimum of the surface free energy. Generally speaking, the growth of lamellar eutectic patterns depends on the orientation of the crystals in a given eutectic grain via the effect of the interfacial anisotropy of the interphase boundaries [6, 7]. This statement has been formalized theoretically a few years ago [8]. A semi-empirical theory of the lamellar-locking phenomenon has been proposed, with a clear experimental and numerical support [9–13]. Experimentally, however, it has been observed in metallic ingots that the relative orientation of the eutectic crystals often departs from a strict coincidence. In addition, the crystal orientation slightly varies inside a eutectic grain (see, e.g., Refs. [14, 15]). Both the origin of this mosaicity, and its consequences on the growth dynamics are far from being known and understood. The first point is a specifically experimental question. The second point can be addressed from a more general viewpoint. This is the aim of the present study.

In this short paper, we report on the first, mostly preliminary results of a numerical investigation of the dynamics of tilted-lamellar growth patterns in the presence of a finite mosaicity. We used a dynamic boundary-integral code in two dimensions [16], using simplified interfacial-anisotropy functions attached to the interphase boundaries [11]. In a sharp-interface formulation of the coupled eutectic growth problem, the interfacial anisotropy intervenes in the local equilibrium at trijunctions, at which the interphase boundary and the two solid-liquid interfaces meet. A reference situation consists of a periodic lamellar pattern with a given interfacial anisotropy, described with suitable functions and parameters. It is now known that the system can reach a steady-state with tilted lamellae exhibiting a constant and uniform tilt angle [8]. In this view, a mosaicity is equivalent to a slight variation in space, that is, from one interphase boundary to another, of the interfacial-anisotropy parameters. The question is then that of the existence and the characterization of a steady-state regime in a mosaic eutectic grain.

II. METHODS

The numerical code has been initially developed by Karma and Sarkissian for the simulation of lamellar eutectic patterns in two dimensions, considering an isotropic system [16]. It is based on a dynamic boundary-integral (BI) method that permits, within some approximations, to calculate the shape and the time evolution of the (sharp) solid-liquid interface without computing the solute diffusion field in the bulk liquid. It is quantitatively accurate, as confirmed by direct comparisons

* akamatsu@insp.jussieu.fr

between BI simulations and in situ experimental observations [17]. An important point, relevant to the present study, is that the motion of the trijunctions is treated separately, in a way that easily allows one to introduce an anisotropy of the interphase boundaries. In Refs. [11, 17], for fundamental demonstration purposes, the BI simulations were performed by considering a single pair of lamellae in a periodic pattern. A given anisotropy function was assigned to the two interphase boundaries in the simulation box, and the two trijunctions behaved similarly. In the following, the simulation box (of width W) was containing 2 or 8 pairs of lamellae. Please note that W will be used as a unit of length, and W/V as a unit of time (V is the solidification velocity). The duration of a simulation, using a standard PC, was of about 30 min for 2 lamella pairs, and several days for 8 lamella pairs.

The physical parameters were those of the CBr_4-C_2Cl_6 alloy at a concentration of 0.137 (molar fraction of C_2Cl_6), which nearly corresponds to a volume fraction of the β phase in the solid $\eta \approx 0.49$ [16, 17]. The control parameters correspond to a solidification velocity V of 1 μms^{-1}, a temperature gradient G of 110 Kcm^{-1}, and a lamellar spacing λ equal to the value of the minimum-undercooling spacing $\lambda_m \approx 13.9$ μm.

III. RESULTS

Addressing the problem of the solidification of a mosaic eutectic grain obviously imposes to consider a larger system than a single pair of lamellae. In the simplest situation, as regards both geometrical and computational constraints, the simulated system consists of two pairs of lamellae. Let us call α and β the two eutectic solid phases. The repeat unit in a lamellar eutectic growth pattern consists of a pair of α and β platelet-like crystals. A simplistic mosaic, yet periodic system can be constructed by considering a unit cell made of an arrangement of the type $\alpha\beta_1\alpha\beta_2$ with the β-phase crystals β_1 and β_2 presenting a slight misorientation with each other, while the orientation of the α -phase crystals remains uniform (a larger system will be also considered later on in this paper). Then there are two kinds of interphase boundaries, namely the β_1-α and β_2-α interfaces –which have the same properties as the α-β_1 and α-β_2 interfaces, respectively, since we consider centrosymmetric crystals. The interfacial anisotropy (γ-plot) of both α-β_1 and α-β_2 interphase boundaries was described with a simple cos2θ function. More precisely, the surface energies $\gamma^{1,2}$ of the α-$\beta_{1,2}$ interphase boundaries are given by:

$$\gamma^{1,2}(\theta) = \gamma_0[1 - \epsilon^{1,2}\cos2(\theta^{1,2} - \theta_R^{1,2})], \qquad (1)$$

where $\theta^{1,2}$ are the current inclination angles of the α-$\beta_{1,2}$ interphase boundaries with respect to the main solidification axis $\mathbf{z}$, $\epsilon^{1,2}$ the anisotropy coefficients, and $\theta_R^{1,2}$ the local orientation angle of the γ-plots. The coefficient γ_0 was set to 1 (see Ref. [17]). For the sake of simplicity, we set $\epsilon^1 = \epsilon^2 = 0.2$. The misorientation angle $\theta_R^1 = 20$ deg was kept constant, while θ_R^2 was varied, from one simulation to another, from 0 to 30 deg. Figure 1a shows the evolution of the $\alpha\beta_1\alpha\beta_2$ pattern for $\theta_R^2 = 0$. It can be seen that, after a transient regime, the four interphase boundaries are tilted, and parallel with each other, which signals a steady-state growth regime.

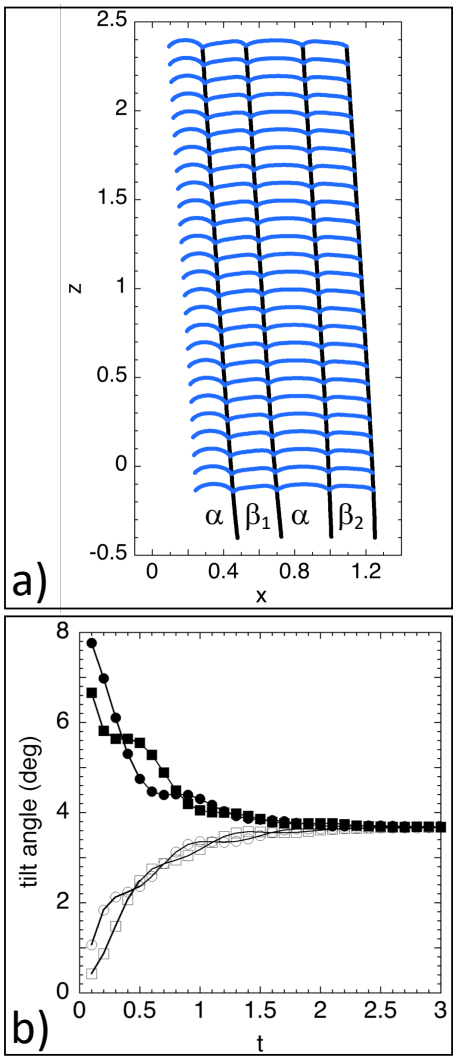

FIG. 1. a) Dynamic BI simulation of a eutectic growth pattern made of two pairs of lamellae of the type $\alpha\beta_1\alpha\beta_2$ with a nonuniform anisotropy (blue lines: solid-liquid interfaces; black lines: interphase boundaries). b) Variation of the lamellar tilt angle θ_t as a function of dimensionless time $t = \hat{t}V/W$, where $\hat{t}$ is the real time. See text for details.

This is more clearly evidenced in the graph of Fig. 1b, in which the tilt angle θ_t of the four interphase boundaries are reported as a function of time t. It can be seen that the tilt angle of the two interphase boundaries with $\theta_R^1 = 20$ deg (on the left of the pattern) decreases,

starting from a relatively large value of θ_t. On the opposite, the tilt angle of the two interphase boundaries with $\theta_R^2 = 0$ deg (on the right of the pattern) increases from a θ_t value close to zero. Let us remark that the initial values of θ_t, and the details of the transient depend on the initial guessed shape of the pattern. The four tilt angles eventually converge to a unique, constant value θ_{mos} (the subscript "mos" refers to "mosaic") of about 3.7 deg. A major feature is that the lamellae present different widths, the trijunctions are not at the same z positions, and the solid-liquid interfaces present symmetry broken shapes with asymmetry factors of alternating signs between neighboring lamellae. Nevertheless, the total volume fraction of the β phase remains equal to ≈ 0.49, as expected in steady-state.

Steady-state patterns with qualitatively similar characteristics were observed for the various values of θ_R^2 explored in this study. The variation of the converged tilt angle θ_{mos} as a function of θ_R^2 is shown in the graph of Fig. 2. The value of the steady-state tilt angle $\theta_{st}(\theta_R)$ in a uniform eutectic grain, extracted from BI simulations of a single lamella pair with the same physical parameters as in Fig. 1, is also reported in the graph. With no surprise, θ_t^m and $\theta_t(\theta_R)$ are equal for $\theta_R^2 = \theta_R^1 = 20^o$. For other values of θ_R^2 below or above θ_R^1, θ_{mos} takes an intermediate value between $\theta_{st}(\theta_R^1 = 20^o)$ and $\theta_{st}(\theta_R^2)$.

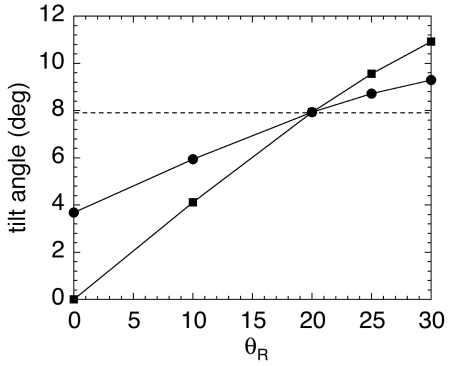

FIG. 2. Lamellar tilt angle as a function of the orientation angle θ_R. Disks: steady-state angle θ_{mos} in mosaic patterns of the same kind as in Fig. 1 as a function of θ_R^2. Squares: steady-state tilt angle θ_{st} in a uniform system. Dotted line: value of the steady-state tile angle θ_{st} for a uniform eutectic grain with $\theta_R = 20^o$.

For a more realistic representation of a mosaic eutectic grain, we performed a BI simulation with 8 lamella pairs. The anisotropy functions were of the same form as in Eq. 1. We set a "random" distribution of both the anisotropy coefficients ϵ_i and θ_R^i (the $i = 1, ..., 16$ number serving as a label for the interphase boundaries in the pattern) about average values $< \epsilon >$ and $< \theta_R >$ of about 0.2 and 2^o, respectively. The departure of ϵ_i (θ_R^i) from $< \epsilon >$ ($< \theta_R >$) was less than about 25% (10%). The mosaic pattern at the end of the simulation (over a length of about $7W$) is shown in Fig. 3a. The image does not present any spectacular feature –the converged tilt angle ($\approx 0.66^o$) is small because $< \theta_R >$ is small as well– but it brings a quite convincing piece of demonstration. The graph in Figs. 3b shows the evolution in time of the spacing distribution $\lambda(x)$. It can be seen that the spacing in the lamellar pattern is slightly nonuniform. Nevertheless, the $\lambda(x)$ curve converges toward a fixed profile in a reference frame drifting with the tilted-lamellar pattern. The graph in Fig. 3c shows the distribution of θ_{mos}^i as the function of the label i of the interphase boundaries (more or less equivalent to the x position). It is essentially flat, which, again, demonstrates that the system reached a steady-state. This appears even more clearly when comparing the value of θ_{mos}^i to that of the steady-state tilt angle θ_{st}^i that was calculated for periodic patterns with a uniform anisotropy of the same kind as the interphase boundary numbered i.

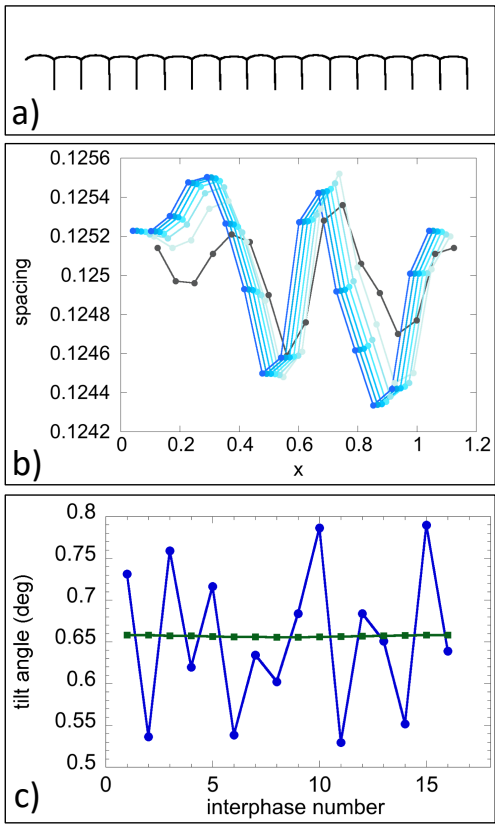

FIG. 3. Dynamic BI simulation of 8 pairs of lamellae. a) Final pattern in steady-state. b) Spacing λ as function of the space variable x for different times (dimensionless time interval: 1.25) during the simulation. Dark-grey data: initial distribution. Colored data: time increases from lighter to darker blue profiles. c) Lamellar tilt angle as a function of the interphase boundary label i. Green: θ_{mos}^i (measured from the pattern in a). Blue: θ_{st}^i.

IV. CONCLUSION

In this study, we performed BI numerical simulations of mosaic-like lamellar eutectic patterns in a realistic alloy. We used smooth anisotropy functions, and more or less steep spatial variations of their parameters. Simulations of a 2-pair lamellar array were used to show the existence of, and provide a first characterization of basic steady-state shapes in the presence of spatially nonuniform anisotropy functions. A simulation with 8 lamella pairs with a random mosaicity also evidences, at least punctually, that a crystallographically imperfect lamellar-eutectic grain can grow with a uniform lamellar tilt, but a nonuniform spacing distribution. Further simulations are needed for a deeper insight into larger systems with a more realistic mosaicity. It will be of great use to compare the simulated growth dynamics and microstructures with experimental observations [18].

ACKNOWLEDGEMENT

We thank A. Karma and A. Sarkissian for sharing with us their original BI code.

[1] K. A. Jackson & J. D. Hunt, Lamellar and rod eutectic growth, Trans. Metall. Soc. AIME, 236 (1966) 1129-1142.
[2] J. A. Dantzig & M. Rappaz, Solidification, 2nd Edition, EPFL Press, Lausanne (2016).
[3] S. Akamatsu & M. Plapp, Eutectic and peritectic solidification patterns, Current Opinion in Solid State and Materials Science, 20 (2016) 46.
[4] L. M. Hogan, R. W. Kraft & F.D. Lemkey, Eutectic grains, Adv. Mater. Res., 5 (1971) 83-126.
[5] U. Hecht, V.T. Witusiewicz, A. Drevermann & S. Rex, Orientation relationship in univariant Al-Cu-Ag eutectics, Trans. Indian Inst. Met., 58 (2005) 545-551.
[6] B. Caroli, C. Caroli, G. Faivre & J. Mergy, Lamellar eutectic growth of CBr4-C2Cl6: effect of crystal anisotropy on lamellar orientations and wavelength dispersion, J. Cryst. Growth, 118 (1992) 135-150.
[7] K. Kassner & C. Misbah, Coupling between crystalline anistropy and spontaneous parity breaking in lamellar eutectic growth, Phys. Rev. A, 45 (1992) 7372-7384.
[8] S. Akamatsu, S. Bottin-Rousseau, M. Şerefoğlu & G. Faivre, A theory of thin lamellar eutectic growth with anisotropic interphase boundaries, Acta Mater., 60 (2012) 3199-3205.
[9] S. Akamatsu, S. Bottin-Rousseau, M. Şerefoğlu & G. Faivre, Lamellar eutectic growth with anisotropic interphase boundaries: Experimental study using the rotating directional solidification method, Acta Mater., 60 (2012) 3206-3214.
[10] S. Bottin-Rousseau, O. Senninger, G. Faivre & S. Akamatsu, Special interphase orientation relationships and locked lamellar growth in thin In-In_2Bi eutectics, Acta Mater., 150 (2018) 16-24.
[11] S. Ghosh, A. Choudhury, M. Plapp, S. Bottin-Rousseau, G. Faivre & S. Akamatsu, Interphase anisotropy effects on lamellar eutectics: a numerical study, Phys. Rev. E, 91, 022407 (2015).
[12] Z. Tu, J. Zhou, L. Tong & Z. Guo, A phase-field study of lamellar eutectic growth with solid-solid boundary anisotropy, J. Cryst. Growth, 532 (2020) 125439.
[13] Z. Tu, J. Zhou, Y. Zhang, W. Li & W. Yu, An analytic theory for the symmetry breaking of growth-front in lamellar eutectic growth influenced by solid-solid anisotropy, J. Cryst. Growth, 549 (2020) 125851.
[14] I. G. Davies & A. Hellawell, Phase orientations in the lamellar and non-lamellar regions of the Al-$CuAl_2$ eutectic alloy, Phil. Mag., 20 (1970) 1255-1259
[15] U. Hecht, V.T. Witusiewicz & A. Drevermann, Coupled growth of Al-Al2Cu eutectics in Al-Cu-Ag alloys, IOP Conference Series: Mat. Sci. Eng., 27 (2012) 012029.
[16] A. Karma & A. Sarkissian, Morphological instabilities of lamellar eutectics, Met. Trans. A, 27 (1996) 635-656.
[17] S. Akamatsu & S. Bottin-Rousseau, Numerical simulations of locked lamellar eutectic growth patterns, Metal. Mater. Trans. A, 52 (2021) 4533-4545.
[18] S. Bottin-Rousseau, M. Medjkoune, O. Senninger, L. Carroz, R. Soucek, U. Hecht & S. Akamatsu, Locked-lamellar eutectic growth in thin Al-Al2Cu samples: in situ directional solidification and crystal orientation analysis, J. Cryst. Growth, 570 (2021) 126203.